Geomechanics and Engineering, *Vol. 19, No. 6 (2019) 533-542*
DOI: https://doi.org/10.12989/gae.2019.19.6.533

Strain rate effects on soil-geosynthetic interaction in fine-grained soil

Maryam Safa[1], Amin Maleka[2], Mohammad-Ali Arjomand[3], Masoud Khorami[4] and Mahdi Shariati*[5,6]

[1]Institute of Research and Development, Duy Tan University, Da Nang 550000, Vietnam
[2]Department of Civil Engineering, Faculty of Engineering, Roudehen Branch, Islamic Azad University, Roudehen, Iran
[3]Faculty of Civil Engineering, Shahid Rajaee Teacher Training University, Tehran, Iran
[4]Department of Civil Engineering, Faculty of Engineering, Central Branch, Islamic Azad University, Tehran, Iran
[5]Division of Computational Mathematics and Engineering, Institute for Computational Science, Ton Duc Thang University, Ho Chi Minh City, Vietnam
[6]Faculty of Civil Engineering, Ton Duc Thang University, Ho Chi Minh City, Vietnam

(Received April 15, 2019, Revised November 12, 2019, Accepted December 14, 2019)

Abstract. Geosynthetic reinforced soil method in coarse-grained soils has been widely used in last decades. Two effective factors on soil-geosynthetic interaction are confining stresses and loading rate in clay. In terms of methodology, one pull-out test with four different strain rates, namely 0.75, 1.25, 1.75 and 2.25 mm/min, and three different normal stresses equal to 20, 50 ,and 80 kg have been performed on specimens with dimensions of 30×30×17 cm in the saturated, consolidated condition. The obtained results have demonstrated that activation of geosynthetic strength at contact surface depends on the applied stress. In addition, the increase in normal stress would increase the shear strength at contact surface between clay and geogrid. Moreover, it is concluded that the strain rate increment would increase the shear strength.

Keywords: reinforced soil; saturated and consolidated soil; geosynthetic; strain rate; pull-out test

1. Introduction

Reinforced soil is an approach to solve the problem of soils with low shear strength through reinforcement. Reinforcements can carry shear forces from soil to reinforcer using soil friction. Geosynthetics are one type of soil reinforcements in reducing the horizontal displacements of soil structures and increasing the overall stability. Therefore, there is a need to study the effective parameters on the interaction of contact surface between geosynthetic and soil. Considering the friction angle of contact surface (δ) and cohesion (C_a) are very important for designing of soil structures. To study the failure modes, two tests namely direct shear test and pull-out test have been conducted (Trung *et al.* 2019b, Xie *et al.* 2019). Soil and concrete are the same problems in shear and tensile forces, where the proposed reinforcing systems have been introduced to mitigate this problem. (Toghroli *et al.* 2017, Heydari *et al.* 2018, Hosseinpour *et al.* 2018, Ismail *et al.* 2018, Nasrollahi *et al.* 2018, Nosrati *et al.* 2018, Paknahad *et al.* 2018, Shariati *et al.* 2018, Toghroli *et al.* 2018, Wei *et al.* 2018, Ziaei-Nia *et al.* 2018, Toghroli 2015, Davoodnabi *et al.* 2019, Li *et al.* 2019, Luo *et al.* 2019, Milovancevic *et al.* 2019, Sajedi *et al.* 2019, Shao *et al.* 2019a, Shariati *et al.* 2019b, Shi *et al.* 2019b, Suhatril *et al.* 2019, Trung *et al.* 2019a, Xie *et al.* 2019). Different studies have investigated the new methods for soil stabilization and soil protection as lime powder addition, slop generation, or other approaches (Muntohar *et al.* 2012, Afrazi *et al.* 2019, Suhatril *et al.* 2019). Few more studies have been performed to evaluate the interaction parameters of the reinforcement contact surface for various soil types such as clay, low quality embankment materials, and for different conditions such as saturated and unsaturated by using these methods. However, the majority of these studies have focused on the non-cohesive soils such as sand and gravel with less attention to cohesive soils. Several available techniques are employed for data validation in which the best methods have been reported as extreme learning machine (Shariati *et al.* 2019a, Shariati *et al.* 2019d, Trung *et al.* 2019b), genetic programming, neural network (NN) ,and other natural basis functional networks (Mohammadhassani *et al.* 2013, Sari *et al.* 2018, Mohammadhassani *et al.* 2014a, Toghroli *et al.* 2014, Shao *et al.* 2015, Shariati *et al.* 2019e, Shariati 2008, Afrazi *et al.* 2018, Safa *et al.* 2016a, Shahabi *et al.* 2016, Khorramian *et al.* 2017, Sadeghipour Chahnasir *et al.* 2018, Sedghi *et al.* 2018, Shao *et al.* 2018, Shariat *et al.* 2018, Katebi *et al.* 2019, Milovancevic *et al.* 2019), also finite element and finite strip methods have been proved as a reliable data authentication and prediction (Sinaei *et al.* 2012, Sharafi *et al.* 2018a, Sharafi *et al.* 2018b, Sharafi *et al.* 2018c, Sharafi *et al.* 2018d, Kildashti *et al.* 2019, Mahdi Shariati 2019, Shao *et al.* 2019b, Shi *et al.* 2019a, Taheri *et al.* 2019, Mortazavi *et al.* 2020). In this study, the utilized soil is Kaolinite that passes from the sieve number 10 with a liquid limit as 53, also the used geosynthetic is CE121 geogrid. All samples are in the thickness of 17 cm and are tested 24 hours after saturation in order to provide consolidation conditions. The optimum moisture is 19%, also the maximum dry specific gravity derived from the

∗Corresponding author, Ph.D.
E-mail: shariati@tdtu.edu.vn

ISSN: 2005-307X (Print), 2092-6219 (Online)

standard proctor test is 1.654 gr/cm^3.

2. Theoretical basis

Depending on the reinforcement type and properties that provided various tests to improve this interaction, the soil-structure interaction is rigorously significant for designing and performance of reinforced soil structures. Niemiec (2005) has performed pull-out tests over three different soil as sand, silica, and clay by using three different geogrid with strength of 0.36, 35, and 120 kN/m. The results have illustrated that:

a) By increasing the normal stress, the failure shear stress would be enhanced.

b) The internal friction angle is increased when the geosynthetic strength grows.

c) Generally, the increment of clay content of soil leads to the friction angle increment.

d) The increment of clay content of soil has also increased cohesion.

e) The failure shear strength is reduced when the clay content of soil is increased (Shariati *et al.* 2019d).

Abdi *et al.* (2009) has improved the strength of contact surface between geogrid and the fine-grained soil using a thin layer high strength grained material around the reinforcement. Accordingly, a large-scale direct shear test (specimen dimension of 30×30×20 cm) is used to evaluate the parameters of friction surface for three types of geogrids and two types of clay and silica sand, as coarse-grained materials. In their study, Abdi *et al.* (when) has evaluated the effects of different factors such as sand grain size, moisture percentage, share of crossed geogrids woof, tensile strength of geogrids, and clay density on the contact surface parameters. One pull-out test by modifying direct shear test set-up has been performed to compare the mentioned factors. The obtained results have demonstrated that by increasing the thickness of sand layer around geogrid, the shear strength of contact surface has been gradually increased until reaching an optimum value. In addition, it is concluded that the increment of sand grains' size could enhance the contact surface shear strength, which is due to the increase in inter-locking between sand grains and geogrid surface. Finally, the moisture of sand layers increases the shear strength compared to dry condition. The evaluations have shown that the share of lateral elements of geogrid in direct shear is 10%-12% of total shear strength; also, 15% growth in clay density would cause 45% increase in shear strength. The effects of density over the shear strength are more in higher normal stresses. Increasing the clay density would increase its internal friction angle, which in turn, improve the friction between soil and geogrid elements to enhance the shear strength at contact surface. In another study, Liu *et al.* (2009) has performed many direct shear tests to evaluate the shear strength at contact surface in different soils (sand, gravel and ocher), and PET-yarn (geogrid) geogrids that possesses different tensile strength, void percentage and surface patterns. After studying different methods for the lower box position, it is concluded that the formation in which the lower box is filled with soil and has the same size to the upper box and provided better condition for the interaction between soil and geogrids. Tests have demonstrated that the shear strength at contact surface between the soil and PET-yarn geotextiles are considerably lower than the soil shear strength. The interaction coefficients for Ottawa sand and ocher are reported 0.7 to 0.8. For gravel. This coefficient is 0.9 to 1.05. Furthermore, this study has shown that besides the friction between soil and reinforcement, and the soil internal friction at geogrid panels, the geogrid transverse grooves has 10% share in contact surface shear strength. Thus, it is reported that this share directly depends on the tensile strength of crossed warps and woofs of geogrid, and also has an inverse relation with a void percentage and panel length of geogrid (Saberian *et al.* 2018, Shariati *et al.* 2019b). Anubhav *et al.* (2001) has investigated the interaction among one type of river sand (D_r=70% and D_{85}=0.95 mm) and two type of polyester geotextiles, one fine-spun and other gross-spun. Through the use of direct shear test, it is found that the maximum shear strength for gross-spun geotextiles without void is remarkably higher than the fine-spun geotextiles, even if the fine-spun geotextiles presents higher level of softening (Paknahad *et al.* 2018). Loading rate is an influential factor on the soil-geosynthetic interaction. Therefore, to study the effects of this factor, in the present study, one pull-out test is used for the evaluation of soil-geosynthetic interaction. According to the American Society for Testing and Materials (ASTM D6706) standards, geosynthetic is buried between two layers of soil. Similarly, the horizontal force is applied to geosynthetic and the needed force to pull it out of the soil is recorded. The pull-out strength is derived by dividing the maximum force to the width of specimen.

$$\sigma_N = \sigma_S + \sigma_a \tag{1}$$

Then, the pull out strength applied to geosynthetic is derived from the following relation. For geotextiles, geo-membranes and reinforcing strips Eq. (2) are used, while Eq. (3) is applicable for geogrids and the similar structures.

$$P_r = F_p / W_g \tag{2}$$

$$P_r = F_p \quad X\ n_g \quad / N_g \tag{3}$$

Output data from the tests are depicted as the diagrams of maximum pull out strength versus normal stress and pull out strength versus displacements of specimens. The interaction behavior is defined by the interaction coefficient derived from comparing the soil friction parameters with those interactions between the soil and the reinforcer. Emersleben *et al.* (2004) has proposed the following relations to compute the interaction coefficient (Mohammadhassani *et al.* 2014b).

$$f_{a\,(\sigma_n)} = (\sigma_n * \tan\delta + \Gamma_0) / (\sigma_n * \tan\varphi + C) \tag{4}$$

$$f_{a\,max} = 2*A*f_{a\,(\sigma_n)} * (\sigma_n * \tan\varphi + C) \tag{5}$$

Thus, it is reported that the interaction coefficient is the function of geogrid type, specific gravity of soil, and confining pressure. Also, $f_n(\sigma_n)$ and $f_g(\sigma_n)$ have been reduced by increasing in confining pressure (normal stress), while the soil density raising would enhance them. Due to the impurity, clay has internal friction angle; thus, the following relation is used for calculation of friction angle:

$$C_i = (C_a + \sigma_n * \tan\delta_a) / (C + \sigma_n * \tan\varphi) \qquad (6)$$

In addition, C_a and δ_n are derived from the diagrams of normal stress versus the maximum pull-out force, and f_{max} is calculated by using Eq. (5).

3. Experimental tests

In this study, Kaolinite is used as a fine-grained material; thus, the properties of Kaolinite are evaluated according to ASTM standards (Table 1). Based on the results and Aterberg limits, Kaolinite belongs to CL level (clay with low plasticity) according to USCS*. Adding that for calculation of cohesion and internal friction angle of the utilized clay in pull-out test, direct shear test is also used.

Tested specimens have optimum moisture and a maximum dry density achieved by the standard proctor test. Utilized kaolinite clay is not completely pure and the existence of impurity has caused a non-zero soil internal friction angle. Fig. 1 demonstrates the density of kaolinite as a function of moisture.

In this study, the utilized geosynthetic is geogrid with a commercial name of CE12 distributed by the Moshiran Company (Table 2). In addition, a large-scale direct shear test machine "NO S08P"† is used. Due to the existence of multiple effective parameters and to reach an acceptable conclusion, parameters such as soil type, moisture percentage, number of layers are constantly kept in all the tests. Therefore, the effects of loading rate and consolidation condition are only studied by using specimens with the length and width of 30 cm and two different thickness of 12 and 17 cm. Figs. 2 and 3 demonstrates the shear machine and the shear box with its modifications.

Table 1 Kaolinite properties

Soil type	Description		ASTM standard	Quantity
Kaolinite	Aterberg limits	Liquid limit	ASTM D4318	39.75 %
		Plastic limit	ASTM D4318	18.9 %
		Plastic index	ASTM D4318	20.85 %
	Density	Optimum moisture	ASTM D698	19 %
		Maximum dry density	ASTM D698	1.654 gr/cm^3
	Shear strength	Non-drained cohesion	ASTM D3080	17.45 kPa
		Non-drained internal friction angle	ASTM D3080	16°

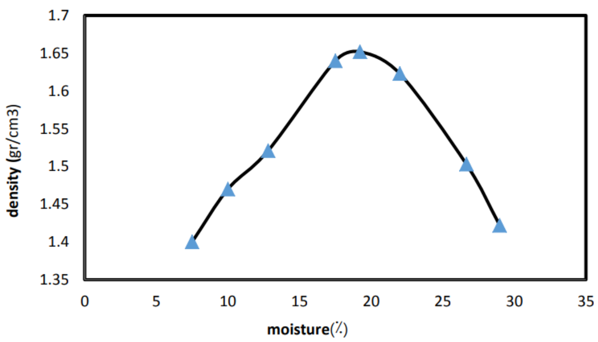

Fig. 1 Standard density of Kaolinite

Table 2 Geogrid properties

Geogrid type	Description	Name/Quantity
CE121	Base material	HDPE
	Cover material	HDPE
	Ultimate tensile strength in longitudinal direction	7.68 kN/m
	Ultimate tensile strength in transvers direction	7.68 kN/m
	Thickness	3 mm
	Panel size	9×7 mm

Fig. 2 The shear box filled with Kaolinite and Geosynthetics

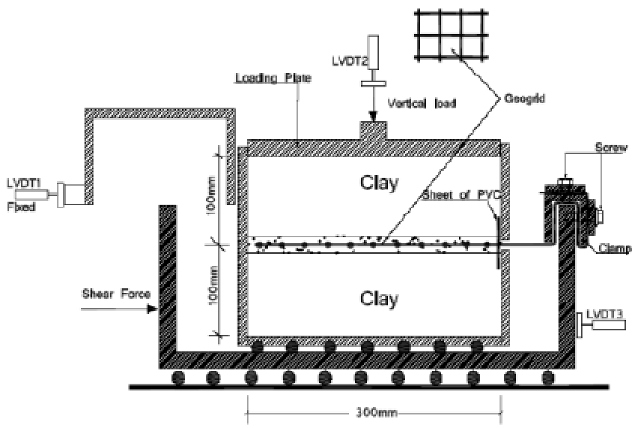

Fig. 3 Test set-up

*unified soil categorization system
†made in Japan

4. Direct shear experiment

In order to study the interaction between soil and geogrid on the contact surface, a large-scale direct shear machine is modified for pull-out test, which is provided the following modifications. The shear boxes placed inside a large box have been re-designed and re-built in a way that a slit with 30 mm length and 6 mm thickness are created in the face of shear box to pull-out the reinforcement (Fig. 2). A clamp was built to connect the reinforcement to the main shear box, in which two screws at its upper face could adjust the clamp height. Three screws were used to fix the clamp position, and there was a metallic rope used for fixing the reinforcement. The upper and lower shear boxes were connected to each other and fixed their places. Later, the outer large box connected to the reinforcement by means of clamp has applied pull-out force by horizontal displacements. To reduce the friction between the lower and outer box, which applies pull-out force, a plate with four roller under the plate were attached to the bottom of lower shear box. To prevent the soil from egressing slit, a grooved PVC sheet was attached to the front of slit.

5. Experiment method

The lower shear box was initially filled with two layers of soils, having an optimum moisture while the soil was compacted by 30 impacts of plastic shaft (10 impacts at center and 5 impacts at each corner). The soil material was compacted in a way that it almost reaches to the maximum

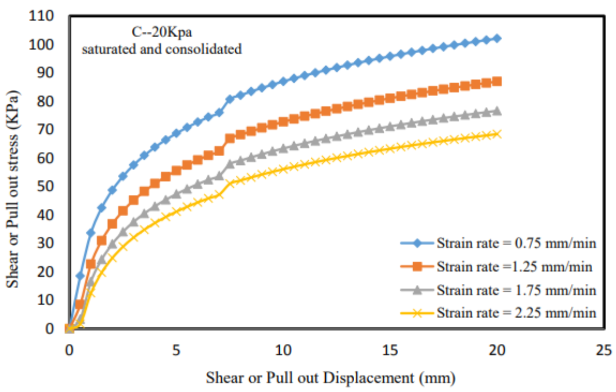

Fig. 4 Pull-out force vs. geogrid displacement at normal stress equal to 20 KPa

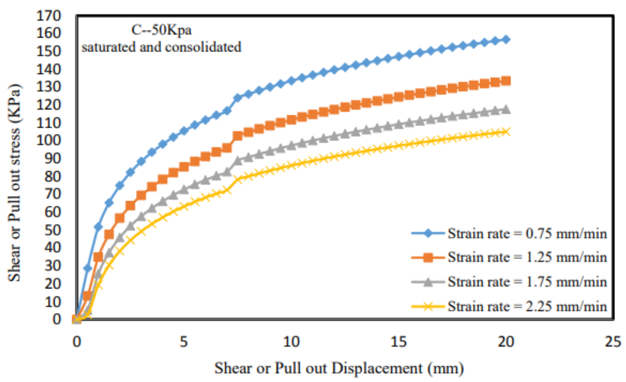

Fig. 5 Pull-out force vs. geogrid displacement at normal stress equal to 50 KPa

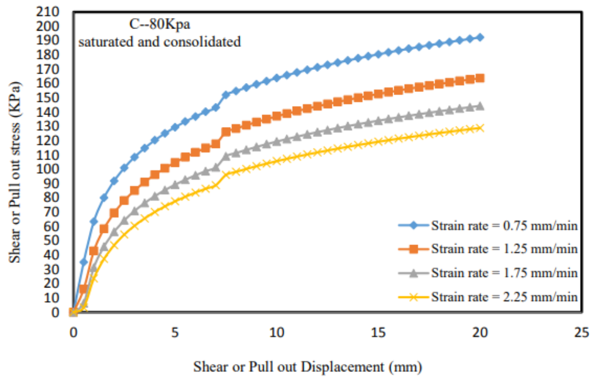

Fig. 6 Pull-out force vs. geogrid displacement at normal stress equal to 80 KPa

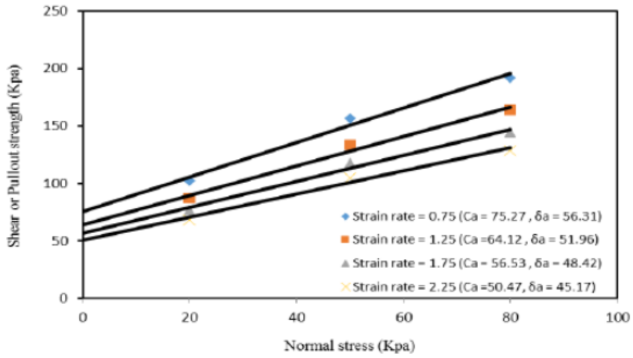

Fig. 7 Maximum pull-out force vs. geogrid normal stress after consolidation

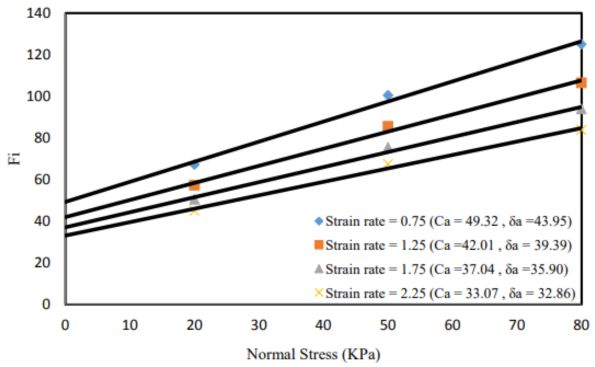

Fig. 8 Fi vs. geogrid normal stress after consolidation

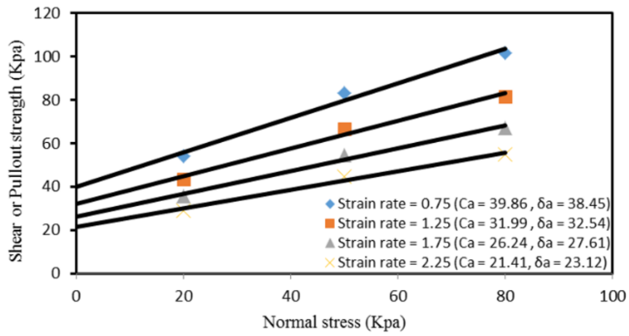

Fig. 9 Maximum pull-out force vs. geogrid normal stress before consolidation

dry density calculated by a standard proctor test. Later, a geogrid specimen with the length to width ratio of 2 were

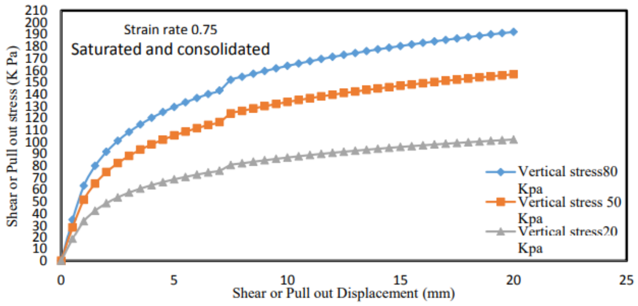

Fig. 10 The pull-out force vs. displacement at the strain rate equal to 0.75 mm/min

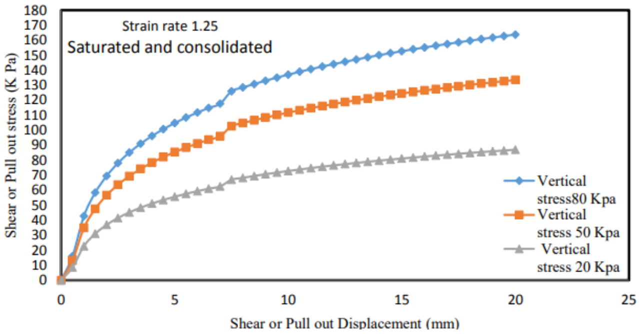

Fig. 11 The pull-out force vs. displacement at the strain rate equal to 1.25 mm/min

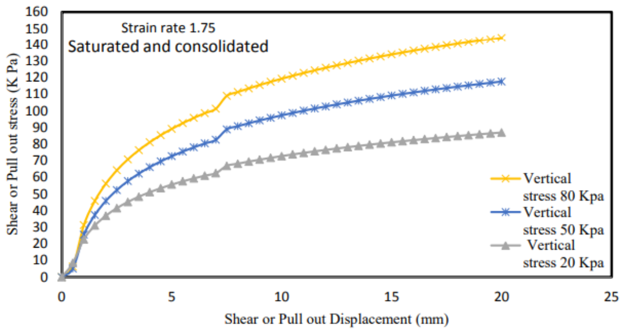

Fig. 12 The pull-out force vs. displacement at the strain rate equal to 1.75 mm/min

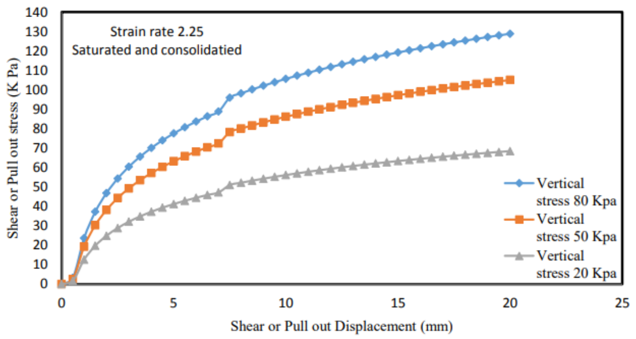

Fig. 13 The pull-out force vs. displacement at the strain rate equal to 2.25 mm/min

connected to the clamp and spread over the lower soil layers in a way that the distance between geogrid and box body was approximately 7.5 cm. Then, the upper box which was filled with a compacted soil is placed over the reinforcement. To perform the test on saturated condition,

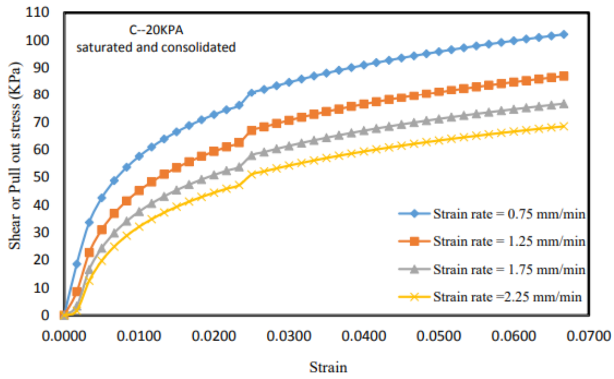

Fig. 14 The pull-out force vs. displacement under the normal stress equal to 20 KPa

porous rocks were placed at the bottom of box and the space between the outer box and shear boxes was filled with water. Later, test was started and the force was applied to the specimens after 24 hours. Different vertical loads as 20, 50 and 80 kN/m^2 were applied to the upper plate of shear box. Using load cell and linear variable differential transformer (LVDTs) are the popular ways to read the experimental data in the different kinds of structural tests (Khorramian *et al.* 2015, Shah *et al.* 2015, Khanouki *et al.* 2016a, Khanouki *et al.* 2016b, Shariati *et al.* 2016a, Shariati *et al.* 2016b, Tahmasbi *et al.* 2016, Khorami *et al.* 2017a, Khorami *et al.* 2017b, Shariati *et al.* 2019d). Two LVDT were placed on the set up to record the applied displacement on geogrid. After starting the displacement machine with the rates of 0.75, 1.25, 1.75 and 2.25 mm/min, the corresponding horizontal force is recorded at 0.5 mm steps. Test is continued to reach the 2 cm lateral displacement in clamp location. This displacement is equal to the displacement at the end of geogrid sample which is connected to the clamp. According to the recorded results and evaluating the width of geogrid specimen in a direction normal to the loading direction, pull out force can be computed. To compute the deformations of reinforcement, the longitudinal location of geogrid nodes was marked by pins. By controlling the location of the pins at the end of the test, approximate displacements of geogrid can be computed. As a result, this method can be used instead of connecting micro strain-gages on geogrid.

6. Results of the direct shear test

The horizontal displacements of geogrid specimen are an influential factor on the parameters of contact surface behavior. To investigate its effects, this section has presented the outcomes of pull-out test performed on saturated and consolidated clay specimens and reinforced by CE121 geogrids. The utilized geogrid has a longitudinal tensile strength of 7.68 KN/m and the specimen are subjected to different normal stresses (20, 50 and 80 KPa) and loaded to achieve different displacement rates of 0.75, 1.25, 1.75 and 2.25 mm/min. Figs 4 to 6 presents the pull-out force versus geogrid displacements, for different normal stresses equal to 20, 50 and 80 KPa, respectively. In these

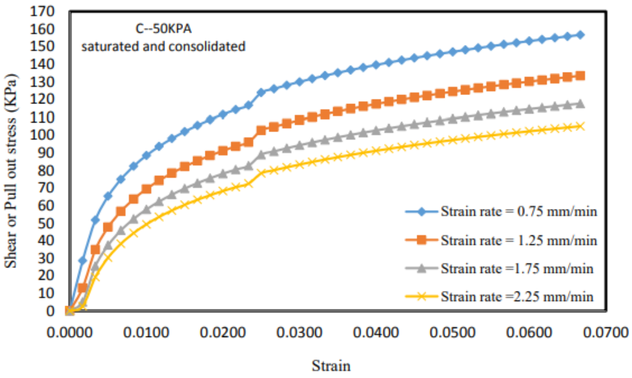

Fig. 15 The pull-out force vs. displacement under the normal stress equal to 50 KPa

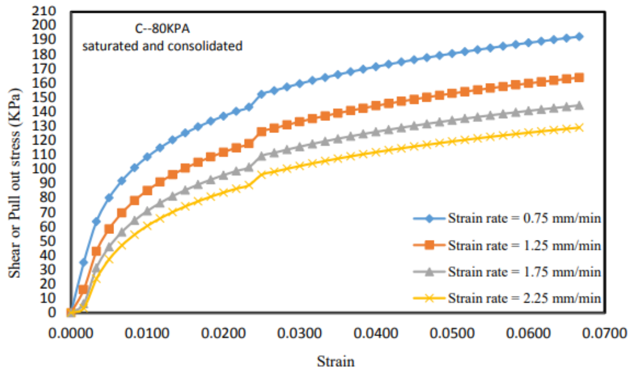

Fig. 16 The pull-out force vs. displacement under the normal stress equal to 80 KPa

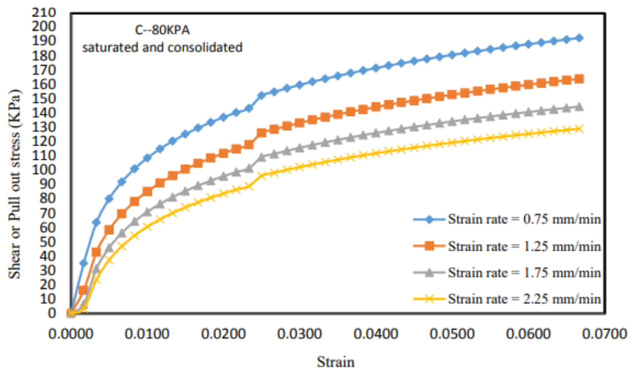

Fig. 16 The pull-out force vs. displacement under the normal stress equal to 80 KPa

Figures, the higher curves are occurred when the strain rate is 0.75 mm/min. Accordingly, increasing the strain rate would reduce the difference between the curves for different strain rates.

Fig. 7 demonstrates the maximum pull-out strength of clay-geogrid specimens. Thus, increasing the strain rate from 0.75 to 2.25 mm/min would reduce the apparent cohesion from 75.27 to 50.47 KN/m and to reduce the apparent friction angle from 56.31 to 45.17 degrees.

However, this reduction is less than the condition of saturation before consolidation, according to Figs 7 and 8, the cohesion reduction in saturated condition before consolidation is 46.29% (Fig. 9), while this reduction after consolidation is only 32.95%. For the friction angle, the reduction before consolidation is 39.87% and after consolidation is 19.79%.

Table 3 Obtained responses for the conducted tests

Test No.	Soil type	Strain rate (mm/min)	Geogrid type	Normal stress (KPa)	Maximum pull-out stress (KN/m^2)	Maximum pull-out force (KN/m)	Strain at the maximum force
1	Clay	0.75	CE121	20	102.12	67.14	0.0133
2	Clay	1.25	CE121	20	86.98	57.19	0.0183
3	Clay	1.75	CE121	20	76.69	50.42	0.0198
4	Clay	2.25	CE121	20	68.47	45.02	0.0208
5	Clay	0.75	CE121	50	156.68	100.44	0.0145
6	Clay	1.25	CE121	50	133.45	85.55	0.0167
7	Clay	1.75	CE121	50	117.66	75.43	0.0183
8	Clay	2.25	CE121	50	105.06	67.35	0.0198
9	Clay	0.75	CE121	80	192.16	124.99	0.0150
10	Clay	1.25	CE121	80	163.68	106.46	0.0175
11	Clay	1.75	CE121	80	144.31	93.86	0.0187
12	Clay	2.25	CE121	80	128.85	83.81	0.0200

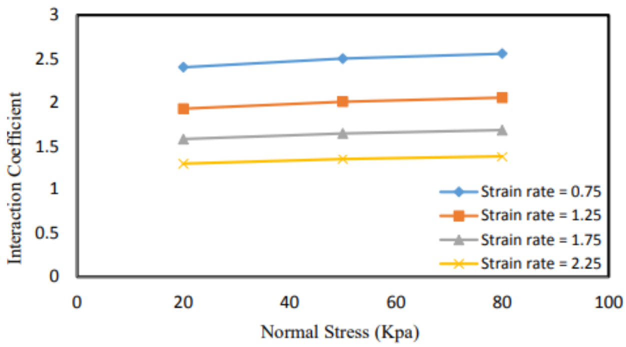

Fig. 17 The interaction coefficients versus normal stress in saturated condition before consolidation

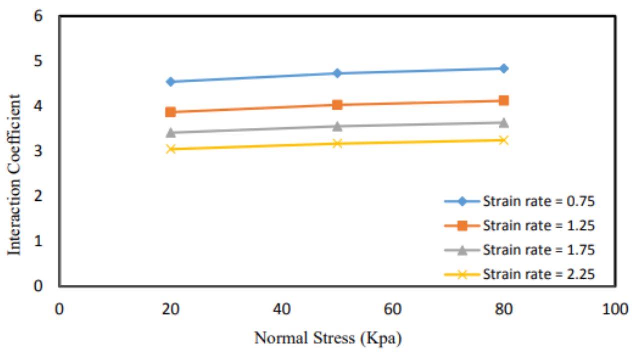

Fig. 18 The interaction coefficients versus normal stress in saturated condition after consolidation

From Fig. 7, the maximum shear strength is occurred at the low strain rates (0.75 mm/min). In addition, the applied normal stress increment would improve the pull-out strength (Figs 10 to 13). Another research has also found that increasing the normal stress has enhanced the failure of shear stress (Hosseinpour *et al.* 2018, Paknahad *et al.* 2018). It's also concluded that increasing the geosynthetic tensile strength has increased the apparent friction angle,

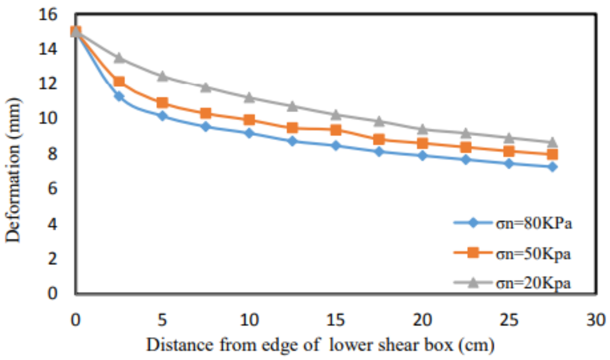

Fig. 19 The deformation variations of CE121 Geogrid along its length regarding the lower shear box

thus the obtained results of this study are in good agreement.

Figs. 14 to 16 show the diagrams of pull-out force versus strain. These curves have demonstrated that the variation of pull-out force is rapid when the strain is below 0.01. After this limit, increasing the strain has not considerably changed the force.

Table 3 presents the obtained responses such as maximum pull-out stresses and forces and the corresponding strains for the conducted tests.

The apparent cohesion and internal friction angle have been computed using the curves of maximum pull-out versus normal stress; hence, the maximum force (f_{max}) are computed by utilizing the Eq. (5). The diagrams depicted in Figs. 17 and 18 show the variation of interaction coefficients as a function of normal stress in the saturated condition (before and after consolidation), respectively. It is evident that at any strain rate, improving normal stress, has increased the interaction coefficients. Furthermore, it can be seen that there is an inverse relation between the interaction coefficient and strain rate. A direct relation between the interaction coefficient and normal stress shows that the CE121 geogrid has acceptable adhesion to clay. In a real condition, the shear failure has been occurred on the surface with the lowest shear strength. Thus, the interaction coefficient cannot be greater than one. Accordingly, the interaction coefficients greater than one has indicated that the contact surface between soil and geogrid can provide the shear strength at least equal to the soil shear strength.

Comparing the optimum moisture with soil, the interaction coefficient in the saturated condition before consolidation is reduced by 26.26% at the strain rate of 0.75 mm/min. This reduction is 34.72, 43.22, and 51.72 at the strain rates of 1.25, 1.75, and 2.25 mm/min, respectively. As previously explained, at the first step of experiment in which the specimen has the maximum dry density and optimum moisture, deformations of geogrid specimen at different points after applying the pull-out force are computed through the evaluation pins (Fig. 19).

The total applied deformation to the connected end of geogrid specimen is 16 mm. According to Fig. 19, it is evident that the deformations at the point of loading are equal to the total applied deformations; therefore, by going further from this point, the deformations are reduced. This trend occurs at any normal stress. In addition, increasing the normal stress applied to the buried length of geogrid would increase its deformations. As a result, according to the nonlinear reduction of deformations along the geogrid specimen, a developed shear stresses in geogrid could be nonlinear.

7. Conclusions

1. The outcomes have shown that the behavior of clay-geogrid is completely hardening, and no softening has been observed during the experiments.

2. The activation of geogrid strength in contact surface depends on the applied vertical stresses. Increasing the vertical stresses would increase the portion of activated geogrid strength.

3. There is an inverse relation between the strain rate and shear strength in a way that the maximum and minimum shear strength have been occurred in the strain rates of 0.75 and 2.25 mm/min, respectively.

4. The geogrid deformation diagram shows that reinforcement system deformation at the connection to clamp is equal to the clamp displacement, while decreased by the raise of the distance from clamp. In addition, the curves show that the geogrid deformations along its buried length have been raised by raising the normal stress value.

References

Afrazi, M. and Rouhanifar, S. (2019), “Experimental study on mechanical behavior of sand-rubber mixtures”, *Modares Civ. Eng. J.*, **19**(4), 83-96 (In Persian).

Afrazi, M., Yazdani, M., Alitalesh, M. and Fakhimi, A. (2018), “Numerical analysis of effective parameters in direct shear test by hybrid discrete – finite element method”, *Modares Civ. Eng. J.*, **18**(3), 13-24 (In Persian).

Arabnejad Khanouki, M.M., Sulong, N.R., Shariati, M. and Tahir, M.M. (2016a), “Investigation of through beam connection to concrete filled circular steel tube (CFCST) column”, *J. Construct. Steel Res.*, **121**, 144-162. https://doi.org/10.1007/s00366-019-00780-7.

Arabnejad Khanouki, M.M., Sulong, N.R., Shariati, M. and Tahir, M.M. (2016b), “Investigation of through beam connection to concrete filled circular steel tube (CFCST) column”, *J. Construct. Steel Res.*, **121**, 144-162. DOI: 10.1016/j.jcsr.2016.01.002.

Davoodnabi, S.M., Mirhosseini, S.M. and Shariati, M. (2019), “Behavior of steel-concrete composite beam using angle shear connectors at fire condition”, *Steel Compos. Struct.*, **30**(2), 141-147. https://doi.org/10.12989/scs.2019.30.2.141.

Heydari, A. and Shariati, M. (2018), “Buckling analysis of tapered BDFGM nano-beam under variable axial compression resting on elastic medium”, *Struct. Eng. Mech.*, **66**(6), 737-748. https://doi.org/10.12989/sem.2018.66.6.737.

Hosseinpour, E., Baharom, S., Badaruzzaman, W.H.W., Shariati, M. and Jalali, A. (2018), “Direct shear behavior of concrete filled hollow steel tube shear connector for slim-floor steel beams”, *Steel Compos. Struct.*, **26**(4), 485-499. https://doi.org/10.12989/scs.2018.26.4.485.

Ismail, M., Shariati, M., Abdul Awal, A.S.M., Chiong, C.E., Chahnasir, E.S., Porbar, A., Heydari, A. and Khorami, M. (2018), “Strengthening of bolted shear joints in industrialized ferrocement construction”, *Steel Compos. Struct.*, **28**(6), 681-

690. https://doi.org/10.12989/scs.2018.28.6.681.
Katebi, J., Shoaei-parchin, M., Shariati, M., Trung, N.T. and Khorami, M. (2019), "Developed comparative analysis of metaheuristic optimization algorithms for optimal active control of structures", *Eng. Comput.*, 1-20. https://doi.org/10.1007/s00366-019-00780-7.
Khorami, M., Alvansazyazdi, M., Shariati, M., Zandi, Y., Jalali, A. and Tahir, M. (2017a), "Seismic performance evaluation of buckling restrained braced frames (BRBF) using incremental nonlinear dynamic analysis method (IDA)", *Earthq. Struct.*, **13**(6), 531-538. http://doi.org/10.12989/eas.2017.13.6.531.
Khorami, M., Khorami, M., Motahar, H., Alvansazyazdi, M., Shariati, M., Jalali, A. and Tahir, M.M. (2017b), "Evaluation of the seismic performance of special moment frames using incremental nonlinear dynamic analysis", *Struct. Eng. Mech.*, **63**(2), 259-268. https://doi.org/10.12989/sem.2017.63.2.259.
Khorramian, K., Maleki, S., Shariati, M. and Sulong, N. R. (2015), "Behavior of tilted angle shear connectors", *PLoS One*, **10**(12), e0144288. https://doi.org/10.1371/journal.pone.0144288.
Khorramian, K., Maleki, S., Shariati, M., Jalali, A. and Tahir, M.M. (2017), "Numerical analysis of tilted angle shear connectors in steel-concrete composite systems", *Steel Compos. Struct.*, **23**(1), 67-85. https://doi.org/10.12989/scs.2017.23.1.067.
Kildashti, K., Samali, B., Mortazavi, M., Ronagh, H. and Sharafi, P. (2019), "Seismic collapse assessment of a hybrid cold-formed hot-rolled steel building", *J. Construct. Steel Res.*, **155**, 504-516. https://doi.org/10.1016/j.jcsr.2019.01.010.
Li, D., Toghroli, A., Shariati, M., Sajedi, F., Bui, D.T., Kianmehr, P., Mohamad, E.T. and Khorami, M. (2019), "Application of polymer, silica-fume and crushed rubber in the production of Pervious concrete", *Smart Struct. Syst.*, **23**(2), 207-214. http://doi.org/10.12989/sss.2019.23.2.207.
Luo, Z., Sinaei, H., Ibrahim, Z., Shariati, M., Jumaat, Z., Wakil, K., Mohamad, E.T. and Khorami, M. (2019), "Computational and experimental analysis of beam to column joints reinforced with CFRP plates", *Steel Compos. Struct.*, **30**(3), 271-280. https://doi.org/10.12989/scs.2019.30.3.271.
Milovancevic, M., Marinović, J.S., Nikolić, J., Kitić, A., Shariati, M., Trung, N.T., Wakil, K. and Khorami, M. (2019), "UML diagrams for dynamical monitoring of rail vehicles", *Physica A Stat. Mech. Appl.*, **531**, 121169. https://doi.org/10.1016/j.physa.2019.121169.
Mohammadhassani, M., Nezamabadi-Pour, H., Suhatril, M. and Shariati, M. (2013), "Identification of a suitable ANN architecture in predicting strain in tie section of concrete deep beams", *Struct. Eng. Mech.*, **46**(6), 853-868. http://dx.doi.org/10.12989/sem.2013.46.6.853.
Mohammadhassani, M., Nezamabadi-Pour, H., Suhatril, M. and Shariati, M. (2014a), "An evolutionary fuzzy modelling approach and comparison of different methods for shear strength prediction of high-strength concrete beams without stirrups", *Smart Struct. Syst.*, **14**(5), 785-809. http://dx.doi.org/10.12989/sss.2014.14.5.785.
Mohammadhassani, M., Suhatril, M., Shariati, M. and Ghanbari, F. (2014b), "Ductility and strength assessment of HSC beams with varying of tensile reinforcement ratios", *Struct. Eng. Mech.*, **48**(6), 833-848. http://dx.doi.org/10.12989/sem.2013.48.6.833.
Mortazavi, M., Sharafi, P., Kildashti, K. and Samali, B. (2020), "Prefabricated hybrid steel wall panels for mid-rise construction in seismic regions", *J. Build. Eng.*, **27**, 100942. https://doi.org/10.1016/j.jobe.2019.100942.
Muntohar, A. S., Widianti, A., Hartono, E. and Diana, W. (2012), "Engineering properties of silty soil stabilized with lime and rice husk ash and reinforced with waste plastic fiber", *J. Mater. Civ. Eng.*, **25**(9), 1260-1270. https://doi.org/10.1061/(ASCE)MT.1943-5533.0000659.
Nasrollahi, S., Maleki, S., Shariati, M., Marto, A. and Khorami, M. (2018), "Investigation of pipe shear connectors using push out test", *Steel Compos. Struct.*, **27**(5), 537-543. https://doi.org/10.12989/scs.2018.27.5.537.
Nosrati, A., Zandi, Y., Shariati, M., Khademi, K., Aliabad, M. D., Marto, A., Mu'azu, M.A., Ghanbari, E., Mahdizadeh, M.B., Shariati, A. and Khorami, M. (2018), "Portland cement structure and its major oxides and fineness", *Smart Struct. Syst.*, **22**(4), 425-432. https://doi.org/10.12989/sss.2018.22.4.425.
Paknahad, M., Bazzaz, M. and Khorami, M. (2018), "Shear capacity equation for channel shear connectors in steel-concrete composite beams", *Steel Compos. Struct.*, **28**(4), 483-494.
Saberian, M., Mehrinejad Khotbehsara, M., Jahandari, S., Vali, R. and Li, J. (2018), "Experimental and phenomenological study of the effects of adding shredded tire chips on geotechnical properties of peat", *Int. J. Geotech. Eng.*, **12**(4), 347-356. https://doi.org/10.1080/19386362.2016.1277829.
Sadeghi Chahnasir, E., Zandi, Y., Shariati, M., Dehghani, E., Toghroli, A., Mohamad, E.T., Shariati, A., Safa, M., Wakil, K. and Khorami, M. (2018), "Application of support vector machine with firefly algorithm for investigation of the factors affecting the shear strength of angle shear connectors", *Smart Struct. Syst.*, **22**(4), 413-424. http://doi.org/10.12989/sss.2018.22.4.413.
Safa, M., Shariati, M., Ibrahim, Z., Toghroli, A., Baharom, S.B., Nor, N.M. and Petkovic, D. (2016), "Potential of adaptive neuro fuzzy inference system for evaluating the factors affecting steel-concrete composite beam's shear strength", *Steel Compos. Struct.*, **21**(3), 679-688 http://dx.doi.org/10.12989/scs.2016.21.3.679
Sajedi, F. and Shariati, M. (2019), "Behavior study of NC and HSC RCCs confined by GRP casing and CFRP wrapping", *Steel Compos. Struct.*, **30**(5), 417-432. https://doi.org/10.12989/scs.2019.30.5.417.
Sari, P. A., Suhatril, M., Osman, N., Mu'azu, M., Dehghani, H., Sedghi, Y., Safa, M., Hasanipanah, M., Wakil, K. and Khorami, M. (2018), "An intelligent based-model role to simulate the factor of safe slope by support vector regression", *Eng. Comput.*, **35**(4), 1521-1531. https://doi.org/10.1007/s00366-018-0677-4.
Sedghi, Y., Zandi, Y., Toghroli, A., Safa, M., Mohamad, E.T., Khorami, M. and Wakil, K. (2018), "Application of ANFIS technique on performance of C and L shaped angle shear connectors", *Smart Struct. Syst.*, **22**(3), 335-340. http://doi.org/10.12989/sss.2018.22.3.335
Shah, S.N.R., Sulong, N.R., Shariati, M. and Jumaat, M.Z. (2015), "Steel rack connections: identification of most influential factors and a comparison of stiffness design methods, *PloS one*, **10**(10), e0139422. https://doi.org/10.1371/journal.pone.0139422.
Shahabi, S.E.M., Sulong, N. H., Shariati, M., Mohammadhassani, M. and Shah, S.N.R. (2016), "Numerical analysis of channel connectors under fire and a comparison of performance with different types of shear connectors subjected to fire", *Steel Compos. Struct.*, **20**(3), 651-669. http://dx.doi.org/10.12989/scs.2016.20.3.651.
Shao, Z. and Vesel, A. (2015), "Modeling the packing coloring problem of graphs", *Appl. Math. Modell.*, **39**(13), 3588-3595. https://doi.org/10.1016/j.apm.2014.11.060.
Shao, Z., Armaghani, D.J., Bejarbaneh, B.Y., Mu'azu, M.A. and Mohamad, E.T. (2019a), "Estimating the friction angle of black shale core specimens with Hybrid-ANN approaches", *Measurement*, **145**, 744-755. https://doi.org/10.1016/j.measurement.2019.06.007.
Shao, Z., Gholamalizadeh, E., Boghosian, A., Askarian, B. and

Liu, Z. (2019b), "The chiller's electricity consumption simulation by considering the demand response program in power system", *Appl. Therm. Eng.*, **149**, 1114-1124. https://doi.org/10.1016/j.applthermaleng.2018.12.121.

Shao, Z., Wakil, K., Usak, M., Heidari, M.A., Wang, B. and Simoes, R. (2018), "Kriging empirical mode decomposition via support vector machine learning technique for autonomous operation diagnosing of CHP in microgrid", *Appl. Therm. Eng.*, **145**, 58-70. https://doi.org/10.1016/j.applthermaleng.2018.09.028.

Sharafi, P., Mortazavi, M., Samali, B. and Ronagh, H. (2018a), "Interlocking system for enhancing the integrity of multi-storey modular buildings", *Autom. Construct.*, **85**, 263-272. https://doi.org/10.1016/j.autcon.2017.10.023.

Sharafi, P., Mortazavi, M., Usefi, N., Kildashti, K., Ronagh, H. and Samali, B. (2018b), "Lateral force resisting systems in lightweight steel frames: recent research advances", *Thin-Walled Struct.*, **130**, 231-253. https://doi.org/10.1016/j.tws.2018.04.019.

Sharafi, P., Rashidi, M., Mortazavi, M., Samali, B. and Ronagh, H. (2018c), "Identification of factors and multi-criteria decision analysis of the level of modularization in building construction", *J. Archit. Eng.*, 24.

Sharafi, P., Rashidi, M., Samali, B., Ronagh, H. and Mortazavi, M. (2018d), "Identification of factors and decision analysis of the level of modularization in building construction", *J. Archit. Eng.*, **24**(2), 04018010. https://doi.org/10.1061/(ASCE)AE.1943-5568.0000313.

Shariat, M., Shariati, M., Madadi, A. and Wakil, K. (2018), "Computational Lagrangian multiplier method using optimization and sensitivity analysis of rectangular reinforced concrete beams", *Steel Compos. Struct.*, **29**(2), 243-256.DOI: http://dx.doi.org/10.12989/scs.2018.29.2.243.

Shariati, M. (2008), "Assessment of building using none-destructive test techniques (ultrasonic Pulse Velocity and Schmidt rebound hammer)", Ph.D. Dissertation, Universiti Putra Malaysia, Serdang, Malaysia.

Shariati, M., Safaei Faegh, S., Mehrabi, P., Bahavarnia, S., Zandi, Y., Masoom, D.R., Toghroli, A., Trung, N.T. and Salih, M.N. (2019), "Numerical study on the structural performance of corrugated low yield point steel plate shear walls with circular openings", *Steel Compos. Struct.*, **33**(4), 569-581. https://doi.org/10.12989/scs.2019.33.4.569.

Shariati, M., Mafipour, M.S., Mehrabi, P., Bahadori, A., Zandi, Y., Salih, M.N.A., Nguyen, H., Dou, J., Song, X. and Poi-Ngian, S. (2019e), "Application of a hybrid artificial neural network-particle swarm optimization (ANN-PSO) model in behavior prediction of channel shear connectors embedded in normal and high-strength concrete", *Appl. Sci.*, **9**(24), 5534. https://doi.org/10.3390/app9245534.

Shariati, M., Mafipour, M.S., Mehrabi, P., Zandi, Y., Dehghani, D., Bahadori, A., Shariati, A., Trung, N.T., Salih, M.N.A. and Poi-Ngian, S. (2019a), "Application of Extreme Learning Machine (ELM) and Genetic Programming (GP) to design steel-concrete composite floor systems at elevated temperatures", *Steel Compos. Struct.*, **33**(3), 319-332. https://doi.org/10.12989/scs.2019.33.3.319.

Shariati, M., Rafiei, S., Zandi, Y., Fooladvand, R., Gharehaghaj, B., Shariat, A., Trung, N.T., Salih, M.N.A., Mehrabi, P. and Poi-Ngian, S. (2019b), "Experimental investigation on the effect of cementitious materials on fresh and mechanical properties of self-consolidating concrete", *Adv. Concrete Construct.*, **8**(3), 225-237. https://doi.org/10.12989/acc.2019.8.3.225.

Shariati, M., Sulong, N.R., Shariati, A. and Khanouki, M.A. (2016a), "Behavior of V-shaped angle shear connectors: experimental and parametric study", *Mater. Struct.*, **49**(9), 3909-3926. https://doi.org/10.1617/s11527-015-0762-8.

Shariati, M., Sulong, N.R., Shariati, A. and Kueh, A.B.H. (2016b), "Comparative performance of channel and angle shear connectors in high strength concrete composites: An experimental study", *Construct. Build. Mater.*, **120**, 382-392. https://doi.org/10.1016/j.conbuildmat.2016.05.102.

Shariati, M., Tahir, M.M., Wee, T.C., Shah, S.N.R., Jalali, A., Abdullahi, M.A.M. and Khorami, M. (2018), "Experimental investigations on monotonic and cyclic behavior of steel pallet rack connections", *Eng. Fail. Anal.*, **85**, 149-166. https://doi.org/10.1016/j.engfailanal.2017.08.014.

Shariati, M., Trung, N.T., Wakil, K., Mehrabi, P., Safa, M. and Khorami, M. (2019d), "Moment-rotation estimation of steel rack connection using extreme learning machine", *Steel Compos. Struct.*, **31**(5), 427-435. https://doi.org/10.12989/scs.2019.31.5.427.

Shi, X., Hassanzadeh-Aghdam, M.K. and Ansari, R. (2019a), "Viscoelastic analysis of silica nanoparticle-polymer nanocomposites", *Compos. Part B Eng.*, **158**, 169-178. https://doi.org/10.1016/j.compositesb.2018.09.084.

Shi, X., Jaryani, P., Amiri, A., Rahimi, A. and Malekshah, E.H. (2019b), "Heat transfer and nanofluid flow of free convection in a quarter cylinder channel considering nanoparticle shape effect", *Powder Technol.*, **346**, 160-170. https://doi.org/10.1016/j.powtec.2018.12.071.

Sinaei, H., Shariati, M., Abna, A.H., Aghaei, M. and Shariati, A. (2012), "Evaluation of reinforced concrete beam behaviour using finite element analysis by ABAQUS", *Sci. Res. Essays* **7**(21), 2002-2009. https://doi.org/10.5897/SRE11.1393.

Suhatril, M., Osman, N., Sari, P.A., Shariati, M. and Marto, A. (2019), "Significance of surface eco-protection techniques for cohesive soils slope in Selangor, Malaysia", *Geotech. Geol. Eng.*, **37**(3), 2007-2014. https://doi.org/10.1007/s10706-018-0740-3.

Taheri, E., Firouzianhaji, A., Usefi, N., Mehrabi, P., Ronagh, H. and Samali, B. (2019), "Investigation of a method for strengthening perforated cold-formed steel profiles under compression loads", *Appl. Sci.*, **9**(23), 5085. https://doi.org/10.3390/app9235085.

Tahmasbi, F., Maleki, S., Shariati, M., Sulong, N.R. and Tahir, M.M. (2016), "Shear capacity of C-shaped and L-shaped angle shear connectors", *PLoS One*, **11**(8), e0156989. https://doi.org/10.1371/journal.pone.0156989.

Toghroli, A. (2015), "Applications of the ANFIS and LR models in the prediction of shear connection in composite beams", Ph.D. Dissertation, The University of Malaya, Kuala Lumpur, Malaysia.

Toghroli, A., Mohammadhassani, M., Suhatril, M., Shariati, M. and Ibrahim, Z. (2014), "Prediction of shear capacity of channel shear connectors using the ANFIS model", *Steel Compos. Struct.*, **17**(5), 623-639. http://dx.doi.org/10.12989/scs.2014.17.5.000.

Toghroli, A., Shariati, M., Karim, M.R.B. and Ibrahim, Z. (2017), "Investigation on composite polymer and silica fume–rubber aggregate pervious concrete", *Proceedings of the 5th International Conference on Advances in Civil, Structural and Mechanical Engineering - CSM 2017*, Zurich, Switzerland.

Toghroli, A., Shariati, M., Sajedi, F., Ibrahim, Z., Koting, S., Mohamad, E.T. and Khorami, M. (2018), "A review on pavement porous concrete using recycled waste materials", *Smart Struct. Syst.*, **22**(4), 433-440. https://doi.org/10.12989/sss.2018.22.4.433.

Trung, N.T., Alemi, N., Haido, J.H., Shariati, M., Baradaran, S. and Yousif, S.T. (2019a), "Reduction of cement consumption by producing smart green concretes with natural zeolites", *Smart Struct. Syst.*, **24**(3), 415-425. https://doi.org/10.12989/sss.2019.24.3.415.

Trung, N.T., Shahgoli, A.F., Zandi, Y., Shariati, M., Wakil, K., Safa, M. and Khorami, M. (2019b), "Moment-rotation prediction of precast beam-to-column connections using extreme learning machine", *Struct*. *Eng*. *Mech*., **70**(5), 639-647. https://doi.org/10.12989/sem.2019.70.5.639.

Wei, X., Shariati, M., Zandi, Y., Pei, S., Jin, Z., Gharachurlu, S., Abdullahi, M.M., Abdullahi, M.M. and Khorami, M. (2018), "Distribution of shear force in perforated shear connectors", *Steel Compos*. *Struct*., **27**(3), 389-399. http://doi.org/10.12989/scs.2018.27.3.389.

Xie, Q., Sinaei, H., Shariati, M., Khorami, M., Mohamad, E.T. and Bui, D.T. (2019), "An experimental study on the effect of CFRP on behavior of reinforce concrete beam column connections", *Steel Compos*. *Struct*., **30**(5), 433-441. http://doi.org/10.12989/scs.2019.30.5.433.

Ziaei-Nia, A., Shariati, M. and Salehabadi, E. (2018a), "Dynamic mix design optimization of high-performance concrete", *Steel Compos*. *Struct*., **29**(1), 67-75. https://doi.org/10.12989/scs.2018.29.1.067.

CC